Molecular simulations of liquid-liquid interfacial properties: Water–*n*-alkane and water-methanol–*n*-alkane systems

José L. Rivera*
Department of Chemical Engineering, University of Tennessee, Knoxville, Tennessee 37996

Clare McCabe
Department of Chemical Engineering, Colorado School of Mines, Golden, Colorado 80401

Peter T. Cummings
Department of Chemistry, Chemical Engineering and Computer Science, University of Tennessee, Knoxville, Tennessee 37996 and Chemical Sciences Division, Oak Ridge National Laboratory, Oak Ridge, Tennessee 37831

(Received 4 July 2002; published 16 January 2003)

Direct molecular dynamics simulations of the liquid-liquid interface of water–*n*-alkane and water-methanol–*n*-alkane systems have been performed in order to study the interfacial properties of these systems. The simulations were carried out using the NERD revised force field of Nath *et al.* for the *n*-alkanes, the simple point charge extended model for water, and the optimized potential for liquid simulations model for methanol. In order to validate the model employed in this work for the *n*-alkanes we calculated the coexisting densities, surface tension, and thickness of the interface for pure *n*-pentane. For all the systems studied the interfacial tension and thickness were calculated at 298.15 K. Our results show that, by adjusting the number of molecules to reproduce the liquid densities in the direct simulation method of the liquid-liquid interface in multicomponent systems, we are able to reproduce available experimental data for interfacial tension. The interfacial thickness is underpredicted and a constant negative deviation of ~ 2.5 Å from the experimental data is usually observed. We find that methanol acts like surfactant when it is added to the water–*n*-alkane mixtures, reducing the interfacial tension of the liquid-liquid ternary system. The interfacial tension results agree quantitatively well for the range of concentrations of methanol studied.

DOI: 10.1103/PhysRevE.67.011603 PACS number(s): 68.05.−n

I. INTRODUCTION

Oil-water and oil-water-surfactant systems are very important in many scientific and technological aspects. Practical applications in biological systems [1], drug delivery [2], food processing [3], and detergents [4], have been the subject of extensive experimental studies in recent years. Of particular relevance is the use of water flooding in enhanced crude oil recovery [4], a procedure which is designed to maintain the reservoir pressure while oil is extracted through the oil well. During water flooding, capillary action causes significant retention of oil behind the flood front. This trapped oil can be recovered using surfactants, which reduce the oil-water interfacial tension by several orders of magnitude, making it feasible to mobilize and recover the oil [4].

Among the properties that can be studied at the interface, two characterize liquid-liquid and vapor-liquid interfaces: interfacial tension (or surface tension for pure component systems), and density profiles (which also describe the interfacial thickness). Several experimental studies at 298.15 K and 1 atm report liquid-liquid interfacial tension for water–*n*-alkane systems [5–7], the vapor-liquid interfacial thickness of pure water [8], long *n*-alkanes (C_{20} and C_{36}) [9], and liquid-liquid interfacial thickness of water–*n*-alkane systems [10,11]. However, measurements at conditions similar to those in an oil reservoir are scarce [12] because of the difficulties performing experiments under such conditions [5]. While predictions of the interfacial tension using equations of state, have been reported, the lack of equations of state which adequately describe phase equilibria of water–*n*-alkane systems, is an impediment to producing accurate results for interfacial properties at the specified conditions [13]. For some water–*n*-alkane systems with less than 12 carbons in the *n*-alkane chain, theoretical predictions of the interfacial thickness using capillary-wave theory [14,15] have produced excellent results. In capillary-wave theory, besides the contribution from the interfacial thickness that corresponds to the intrinsic structure of the interface, there is a second contribution due to the roughness of the interface propagated by thermally excited capillary waves. The contribution due to the intrinsic structure of the interface for water–*n*-alkane systems can be estimated as the radius of gyration of the larger compound of the system [10].

Molecular simulations have been reported in the literature, which investigate the influence of surfactant concentration on the interfacial tension of model Lennard-Jones ternary systems [16,17]. Smit [16] showed that in the model system, the interfacial tension decreases almost linearly with the decrease in the concentration of surfactant at the interface. However, the results in this study were influenced by the size of the system due to the small number of molecules employed. Diaz-Herrera *et al.* [17] studied larger system sizes and concluded that the dependence is not linear. To our knowledge, there are only five simulations reported in the

*Electronic address: jrivera@posgrado.fiq.umich.mx. Present address: Fac. Ing. Quim., University Michoacana SNH, Morelia 58060, Michoacan, Mexico.

literature using realistic potentials for water–*n*-alkane and water-surfactant–*n*-alkane systems. Water–*n*-hexane was studied by Carpenter and Hehre [18], water–*n*-octane by Zhang *et al.* [19], water–*n*-nonane by Michael and Benjamin [20], water–*n*-decane by van Buuren *et al.* [21], and water-monododecyl pentaethylene glycol-*n*-octane by Kuhn and Rehage [22]. Hence it has been shown that using direct molecular dynamics simulations we are able to characterize the interface of a system, though the accuracy of the results will naturally depend upon the accuracy of the potential model employed for each compound and to some extent on the combining rules used to determine the unlike interactions between the molecules in the system. Furthermore, when dealing with polar molecules, consideration needs to be given to the way long-range electrostatic interactions are computed, since they can represent up to 25% of the total value of the interfacial properties [23,24]. However, of the previous simulation studies using realistic potentials, one of them does not specify the method employed to calculate long-range electrostatic interactions [21] and the remainder simply do not account for these interactions [18–20,22]. All prior simulation studies obtained results for the interfacial thickness, which disagree with the available experimental data [10] with relative errors as large as 80% for the simulation with *n*-octane. Only Zhang *et al.* [19] and van Buuren *et al.* [21] actually calculated interfacial tensions; they obtained poor results with an all atom model of *n*-alkanes [19] and the Ryckaert-Bellemans model [25].

In this work, we performed realistic simulations of the water–*n*-alkane and water-methanol–*n*-alkane interface using the Ewald summation technique, which accurately describes the long-range electrostatic interactions. We initially performed simulations to obtain a system at the correct density and compositions in the bulk phases compared to experimental data. The interfacial properties (density profiles, interfacial thickness, and tension) were then calculated from the resulting configurations.

II. SIMULATION DETAILS

We have performed constant number of molecules, volume, and temperature simulations (NVT-MD) of the vapor-liquid and liquid-liquid interfaces to obtain the coexisting densities and interfacial properties (interfacial thickness and surface and interfacial tensions) for pure *n*-pentane, the binary mixtures of water–*n*-alkane, and the ternary mixture of water-methanol–*n*-pentane. All the simulations were carried out using the Verlet algorithm at constant temperature; the time step used was 1 fs. Depending on the *n*-alkane chain length, the simulation cell contained between 150 and 350 *n*-alkane molecules, 100 to 540 water molecules, and 50 to 220 methanol molecules. The simulations were performed at ambient temperature for the liquid-liquid simulations and from 150 to 336 K for the vapor-liquid simulations of pure *n*-pentane.

The potential model parameters used to describe the water, methanol, and *n*-alkane molecules were taken from Refs. [26,27], and [28] respectively. The reader is directed to the original references for details of each potential model. The intermolecular forces due to Lennard-Jones interactions were computed using a spherically truncated potential [29]. The interaction is given by

$$F_{LJ}(r_{iajb}) = \begin{cases} \dfrac{24\epsilon}{r_{iajb}}\left[2\left(\dfrac{\sigma}{r_{iajb}}\right)^{12} - \left(\dfrac{\sigma}{r_{iajb}}\right)^{6}\right] - U_{LJ}(r_C)\,\delta(r_{iajb} - r_C), & r_{iajb} \leqslant r_C \\ 0, & r_{iajb} > r_C, \end{cases} \tag{1}$$

where σ and ϵ are the Lennard-Jones parameters, r_C is the cutoff radius, and r_{iajb} is the distance between site a in molecule i and site b in molecule j. U_{LJ} is the simple Lennard-Jones potential and δ is a delta function, which is approximated by

$$\delta(r_{iajb} - r_C) = \frac{\theta(r_{iajb} - r_C) - \theta(r_{iajb} - r_C - \Delta r)}{\Delta r}, \tag{2}$$

where θ is the unit step function and Δr is a fixed parameter. Using Eq. (1) to compute the interaction forces with a cutoff ratio greater than $4\sigma_{MAX}$ (σ_{MAX} is the largest Lennard-Jones sigma parameter among the values used for the species studied), we can obtain more precise values for the interfacial properties compared to results using spherically truncated and shifted potentials. Sites in the same molecule separated by three or more bonds interact through the potential given in Eq. (1). The Lorentz-Berthelot mixing rules were used for the cross interaction between unlike sites.

The procedure used in this work to simulate liquid-liquid equilibria is the same as that employed to simulate the liquid-vapor interface of one component or multicomponent systems [30,31]. At the beginning of the simulation, molecules are allocated in the center of a parallelepiped cell surrounded by a vacuum in the z direction. The dimensions of the simulation cell vary depending upon the particular system being studied. A typical size of $L_X = L_Y = 31.44$ Å, and $L_Z = 125.76$ Å for liquid-vapor equilibria, and $L_X = L_Y = 31.44$, and $L_Z = 66.81$ Å for liquid-liquid equilibrium was used. The cutoff radius for Lennard-Jones interactions was 15.72 Å. Electrostatic interactions were handled by the Ewald summation technique with a convergence parameter κ of $5.6/L_X$ and a maximum value for the reciprocal lattice vector h_{MAX} of 10. After an equilibration period of 150 ps the average properties were then obtained from an additional simulation run of 600 ps.

The coexistence densities and compositions were obtained following the same procedure described in Ref. [31]. During

the vapor-liquid simulations, a molecular density profile was obtained and fitted to a hyperbolic tangent function [32] in order to obtain the coexistence densities, viz.,

$$\rho(z)=0.5(\rho_L+\rho_V)-0.5(\rho_L-\rho_V)\tanh\left[\frac{z-z_0}{d}\right], \quad (3)$$

where ρ_L,ρ_V are the liquid and vapor densities, z_0 is the position of the Gibbs dividing surface, and d is a parameter related to the thickness of the interface. The thickness of the interface is calculated as the distance along the interface over which the density changes from a value of 10% to 90% of the total density change between the bulk phases, which corresponds to 2.1972 times the value of parameter d [32]. As a result, this thickness is known as the ''10-90'' interfacial thickness; a frequently used alternative thickness is the ''10-50'' interfacial thickness which is defined analogously.

For systems exhibiting liquid-liquid equilibrium, the thickness of the liquid-liquid interface was calculated using the criteria proposed by Senapati and Berkowitz [33], which results in a prediction for the ''10-50'' interfacial thickness. The density profile of each component is fitted to an expression similar to the one used to fit the experimental data in liquid-liquid water–n-alkane systems [10]:

$$\rho_W(z)=0.5\rho_{WB}+\rho_{WB}\,\mathrm{erf}\left[\frac{z-\langle z_W\rangle}{\sqrt{2}t_C}\right], \quad (4)$$

$$\rho_A(z)=0.5\rho_{AB}-\rho_{AB}\,\mathrm{erf}\left[\frac{z-\langle z_A\rangle}{\sqrt{2}t_C}\right], \quad (5)$$

where $\rho_W(z)$ and $\rho_A(z)$ are the density profiles of water and n-alkane, respectively. ρ_{WB} and ρ_{AB} are the water and n-alkane bulk densities, respectively. $\langle z_W\rangle$ and $\langle z_A\rangle$ are the average positions of each interface, t_C is the contribution to the ''10-50'' interface thickness due to thermal fluctuations, and erf is the error function. The intrinsic interfacial thickness t_0 is obtained as $|\langle z_A\rangle-\langle z_W\rangle|$, the difference between the positions of the fitted interfaces.

The surface and interfacial tensions were calculated using the molecular definition of the pressure tensor. The molecular surface tension is defined in terms of the pressure tensor components as [30]

$$\gamma=\frac{L_Z}{2}[\langle P_{ZZ}\rangle-0.5(\langle P_{XX}\rangle+\langle P_{YY}\rangle)], \quad (6)$$

where $P_{\alpha\alpha}$ is the $\alpha\alpha$ element of the pressure tensor. The factor (1/2) outside the bracket takes into account the fact that there are two interfaces in the system. Brackets for each $P_{\alpha\alpha}$ indicate temporal averages. The element $P_{\alpha\alpha}$ of the molecular pressure tensor for additive pair potentials, as is the case of Lennard Jones, is given by

$$VP_{\alpha\alpha}=\sum_i^N m_i(\boldsymbol{v}_i)_\alpha(\boldsymbol{v}_i)_\alpha+\sum_i\sum_{j>i}\sum_a\sum_b(\boldsymbol{r}_{iajb})_\alpha(\boldsymbol{f}_{iajb})_\alpha, \quad (7)$$

where N is the number of molecules, V is the volume of the system, m_i is the molecular mass, $(\boldsymbol{v}_i)_\alpha$ is the velocity of the center of mass in the α direction, $(\boldsymbol{r}_{iajb})_\alpha$ and $(\boldsymbol{f}_{iajb})_\alpha$ are the distance and interaction force between site a in molecule i and site b in molecule j in the α direction. For pure component simulations we can compute long-range corrections to the surface tension due to Lennard-Jones interactions beyond the cutoff ratio [32]. For n-pentane the expression is given by

$$\gamma_{LRC}=12\pi(\rho_L-\rho_V)^2\sum_{a=1}^5\sum_{b=1}^5\epsilon_{ab}\sigma_{ab}^6\int_0^1 ds \times\int_{r_C}^\infty dr\coth\left(\frac{rs}{d}\right)\frac{(3s^3-s)}{r^3}, \quad (8)$$

where ρ_L and ρ_V are the liquid and vapor coexisting densities. ϵ_{ab} and σ_{ab} are the cross Lennard-Jones parameters.

Using the Ewald summation technique, the reciprocal space contribution is not pairwise additive and Eq. (7) cannot be used. The components for the pressure tensor or electrostatic interactions have already been obtained by Alejandre *et al.* [23,30]. For completeness, we give only the basic equations here:

$$VP_{\alpha\beta}=\sum_i\sum_a q_{ia}\sum_{j>i}\sum_b q_{jb}\left[\frac{2}{\sqrt{\pi}}\kappa r_{iajb}\exp(-\kappa^2 r_{iajb}^2)+\mathrm{erfc}(\kappa r_{iajb})\right]\frac{(\boldsymbol{r}_{ij})_\alpha(\boldsymbol{r}_{iajb})_\beta}{r_{iajb}^3}+\frac{2\pi}{V}\times\sum_{\boldsymbol{h}\neq\boldsymbol{0}}Q(h)S(\boldsymbol{h})S(-\boldsymbol{h})\left(\delta_{\alpha\beta}-\frac{2\boldsymbol{h}_\alpha\cdot\boldsymbol{h}_\beta}{h^2}-\frac{\boldsymbol{h}_\alpha\cdot\boldsymbol{h}_\beta}{2\kappa^2}\right)-\sum_i\sum_a(\boldsymbol{r}_{ia}-\boldsymbol{r}_i)_\beta(\boldsymbol{f}_{ia}^\kappa)_\alpha, \quad (9)$$

$$S(\boldsymbol{h})=\sum_i\sum_a q_{ia}\exp(i\boldsymbol{h}\cdot\boldsymbol{r}_{ia}), \quad (10)$$

$$Q(h)=\exp(-h^2/4\kappa^2)/h^2, \quad (11)$$

$$\boldsymbol{f}_{ia}^\kappa=-\frac{4\pi q_{ia}}{V}\sum_{\boldsymbol{h}\neq 0}Q(h)\boldsymbol{h}\times\mathrm{Im}[\exp(-i\boldsymbol{h}\cdot\boldsymbol{r}_{ia})S(\boldsymbol{h})], \quad (12)$$

where $\boldsymbol{h}$ is the reciprocal lattice vector, δ is the Kronecker delta, erfc is the complementary error function, and Im denotes the imaginary part of the complex variable.

III. VAPOR-LIQUID EQUILIBRIUM RESULTS FOR *n*-PENTANE

The potential chosen to model the n-alkanes was validated for interfacial properties through NVT-MD simulations and the results are presented in this section. For the pure n-pentane system the results of the simulations of the coexisting densities, ''10-90'' interfacial thickness and surface tension as a function of temperature are given in Table I.

TABLE I. Simulation results for *n*-pentane. Average liquid density ρ_L, vapor density ρ_V, "10-90" interface thickness t, long-range correction to the surface tension γ_{LRC}, and the total value γ, as function of temperature. Numbers between parentheses indicate the precision of the total values.

T (K)	ρ_L (g/cm^3)	ρ_V (g/cm^3)	t (Å)	γ_{LRC} (mN/m)	γ (mN/m)
150	0.7225	0.0001	2.62 (0.39)	6.39	33.09 (1.60)
200	0.6807	0.0003	3.59 (0.39)	5.42	25.59 (1.33)
270	0.6187	0.0152	6.20 (0.39)	3.85	19.19 (1.15)
336	0.5552	0.0819	9.48 (0.39)	2.44	12.37 (1.38)

Densities and interfacial thickness were obtained from density profiles fitted to Eq. (3). Bulk phases were extended for more than 50 Å with stable interfaces during the simulations. Our calculated densities agree well with experimental data [34] having maximum absolute errors of 0.035 g/cm^3, which are similar to the errors obtained by Nath *et al.* [28] using the Gibbs ensemble Monte Carlo method. Figure 1 illustrates these comparisons.

The results of calculations to determine the 10-90 interfacial thickness as a function of the temperature are shown in Fig. 2(a), where it can be seen that the thickness of the interface grows monotonically with the temperature. The results of this work for *n*-pentane are similar to previously reported results for simulations of *n*-hexane using the optimized potential for liquid simulations OPLS potential [32], however there are no experimental data or theoretical predictions to which we can compare our results. Calculations of the surface tension are shown as a function of the temperature in Fig. 2(b). The agreement with experimental data [35] is excellent in the range of temperatures studied. Long-range corrections represent around 20% of the total value. Therefore, given these results we feel confident in the use of the NERD (after the authors' names [28]) potential to study interfacial properties of multicomponent systems with water and surfactants.

We did not perform similar validation studies for the water molecules as previous simulations results [23,36] for the simple point charge extended model of water show that this model is also suitable for the study of interfacial properties. In particular, Alejandre *et al.* [23] produced predictions using this model, which agree quantitatively well with experimental data for the surface tension and the 10-90 interfacial thickness had an absolute error of $\sim$1.1 Å ($\sim$33%) at 298.15 K if the extrapolated simulation result is compared to a measurement of Matsumoto and Kataoka [37].

IV. LIQUID-LIQUID EQUILIBRIUM RESULTS FOR WATER–*n*-ALKANE SYSTEMS

The NVT-MD simulations of the liquid-liquid interface of water–*n*-alkane binary mixtures were carried out at 298.15 K, without considering the formation of a vapor phase. From previous simulations at this temperature, the amount of vapor in water and *n*-nonane binary mixtures is negligible [20], this being increasingly true for higher molecular weight *n*-alkanes; extrapolations to this temperature of the predicted vapor phase densities in vapor-liquid equilibria for the models employed are around 0.0001, 0.0040, and 0.0025 g/cm^3 for water [23], *n*-pentane, and *n*-decane [28], respectively. Therefore, the formation of stable liquid-liquid-vapor interfaces is not expected.

Liquid-liquid equilibrium simulations were carried out using the same methodology as vapor-liquid simulations, the

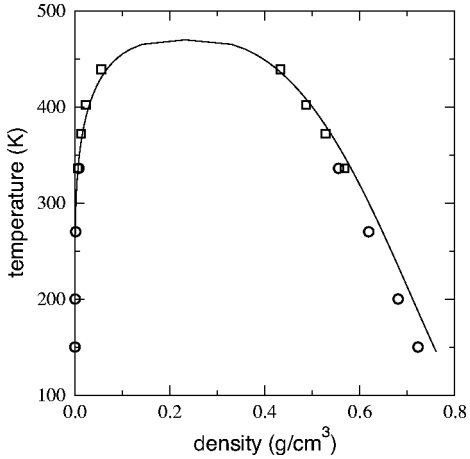

FIG. 1. Liquid-vapor coexistence curve of *n*-pentane. The solid line represents experimental data [34]. Squares and circles represent results from Nath *et al.* [28] and results from this work, respectively.

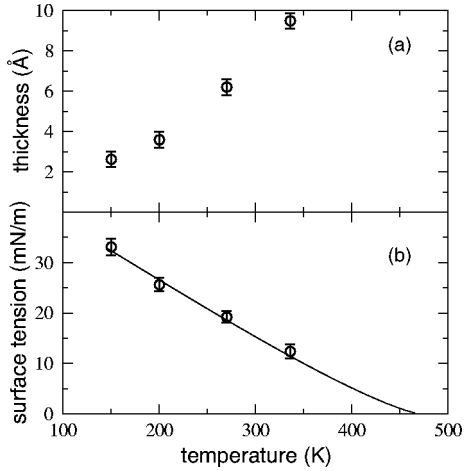

FIG. 2. (a) "10-90" interfacial thickness, and (b) surface tension as function of temperature for *n*-pentane. Solid line represents experimental data from Grigoryev *et al.* [35]. Circles represent results from this work.

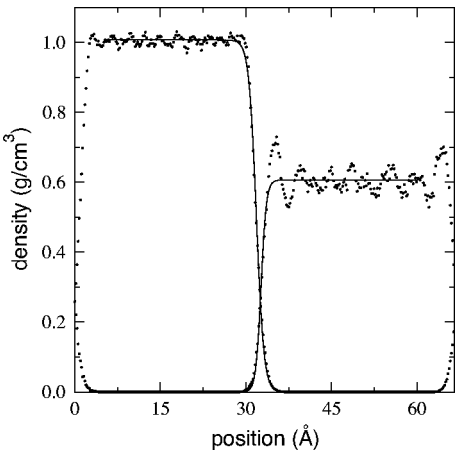

FIG. 3. Density profiles of the liquid-liquid coexistence system water–*n*-pentane at 298.15 K. Left and right dotted lines are for the simulation results of water and *n*-pentane, respectively. Continuous lines represent the fitted profiles to Eqs. (4) and (5).

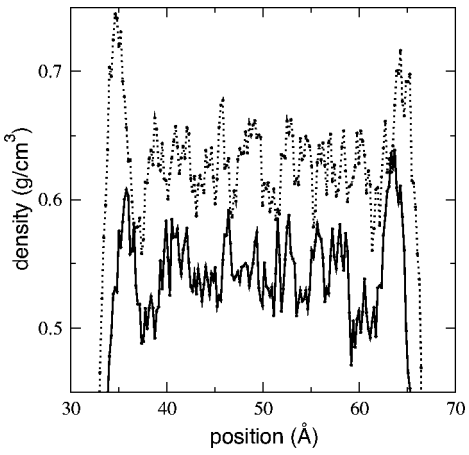

FIG. 4. Density profiles of *n*-pentane in the system water–*n*-pentane at 298.15 K. Continuous and dotted lines are profiles with 152 and 172 molecules of *n*-pentane, respectively.

only difference being that the volume of the simulation cell should have the correct size needed to produce coexisting bulk phases with densities similar to the available experimental data. In this work our goal is not to predict the coexisting bulk densities, but to simulate a system contained in a certain cell volume which will produce bulk phases with densities corresponding to the experimental values. We expect such systems to have a more realistic density profile at the interface and so should produce values of the interfacial properties closer to the experimental data. A simulation cell smaller than the correct cell will produce higher densities or maybe the system will mix with the formation of vapor-liquid equilibrium due to the higher pressure, while a simulation cell greater than the correct cell will provoke a continuous formation and destruction of the interfaces due to the highly repulsive nature of the system components. We can perform such simulations in two ways, either by varying the dimension of one side of the simulation cell or by varying the number of molecules in the system. We choose the second route, where an initial system is equilibrated and the densities in the bulk phases are calculated; molecules are then added or eliminated from the initial system, thus increasing or reducing the bulk densities to values corresponding to experimental data. We note that of the molecules added or removed some of them will go to the interfaces, but most of them will go to the bulk phases. The dimensions of the initial system should consider the fact that we need a simulation cell length bigger than the cutoff ratio in two sides (L_X,L_Y) and the third side should contain at least twice L_X or L_Y (two phases) plus the thickness of the interface, which, for example, can be as big as 3.3 Å for water at 298.15 K [8]. The equilibrated initial density profiles for water–*n*-pentane at 298.15 K are shown in Fig. 3. For this system the bulk phases are extended to $\sim$28 Å and the total interfacial thickness is $\sim$5 Å. The density profile for water is well defined at the interface, in other words we can see clearly where it starts to change in the aqueous phase (water rich) and where it finishes in the organic phase (*n*-alkane rich). For *n*-pentane we can see where the interface finishes in the aqueous phase, but the beginning is not clear because there are molecules of *n*-alkane adsorbed at the interface, hence the density profile for *n*-pentane cannot be fitted by Eq. (3). The profiles fitted by Eqs. (4) and (5) are shown in Fig. 3, and they reproduce the interfacial region well. The ''10-50'' interface thickness was computed using the fitted values of Eqs. (4) and (5).

The system water–*n*-pentane was simulated using a different number of *n*-pentane molecules to see the dependence of the bulk densities on the number of molecules present in the organic phase. In Fig. 4 we can see how the bulk and interfacial densities change when we increase the number of *n*-pentane molecules by 20. As expected, most of the molecules go to the bulk phase, but a fraction of them go to the interface, making it thicker and the peaks representing the molecules adsorbed at the interface higher. The dependence of the bulk densities as a function of the number of *n*-pentanes in the system are shown in Fig. 5, with horizontal lines representing the experimental density of the pure com-

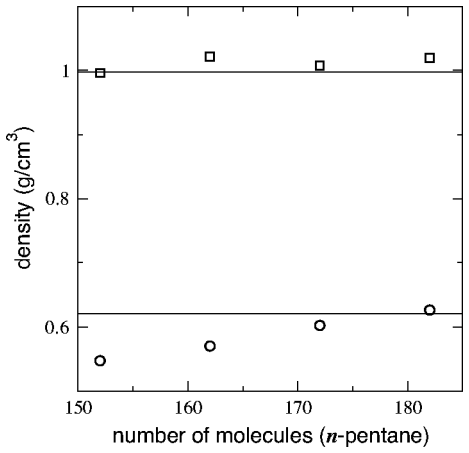

FIG. 5. Density of each liquid phase in the system water–*n*-pentane at 298.15 K as a function of the number of *n*-pentane molecules. Circles and squares represent results from this work for the density of *n*-pentane and water rich phases, respectively. Horizontal lines represent experimental data of pure components [34].

TABLE II. Simulation results for water–*n*-alkane. ''10-50'' intrinsic interface thickness t_0. Interface thickness due to thermal fluctuations t_C. Interfacial tension obtained during simulation γ. Numbers between parentheses indicate the precision of the total values.

System	t_0 (Å)	t_C (Å)	γ (mN/m)
Water–*n*-pentane	0.82	1.06	50.84 (3.16)
Water–*n*-hexane	0.87	1.28	50.91 (2.52)
Water–*n*-heptane	0.91	1.44	51.02 (2.71)
Water–*n*-octane	0.95	1.47	52.10 (2.30)
Water–*n*-nonane	1.16	1.48	53.22 (2.39)
Water–*n*-decane	1.32	1.49	54.04 (2.42)

ponents. The bulk density of water remains almost constant and for *n*-pentane it increases almost linearly with the number of *n*-pentane molecules. Using around 175 molecules of *n*-pentane, we obtained a value for the density in the organic phase which agrees with the experimental data. The net effect of this process of preparing the systems is that at a specified temperature and density of the bulk *n*-alkane rich phase, we obtain the corresponding density of the bulk water phase and interfacial region.

Following the method described above, we simulated systems from water–*n*-pentane through water–*n*-decane. The results of these simulations for interfacial tension and thicknesses are reported in Table II. The results of this work for the calculation of interfacial tensions as a function of the number of carbons in the *n*-alkane chain studied are shown in Fig. 6. Experimental data for water–*n*-pentane from Matsubara *et al.* [7], and for the remaining systems from Mitrinovic *et al.* [10] are also shown. The simulation data follow the same general trend as the experimental data; the interfacial tension increases slightly with increasing the chain length in the *n*-alkane.

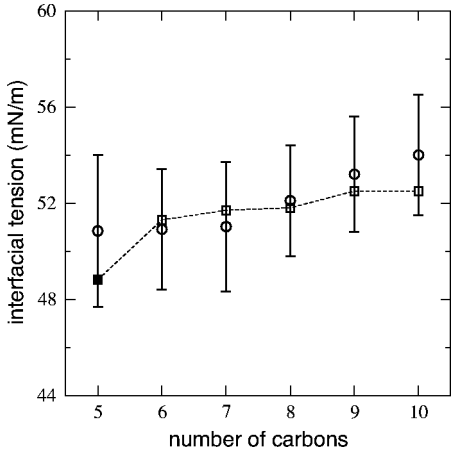

FIG. 6. Interfacial tension of the liquid-liquid water–*n*-alkane systems as function of the number of carbons in the *n*-alkane molecule at 298.15 K. Filled and open squares represent experimental data from Matsubara *et al.* [7] and Mitrinovic *et al.* [10], respectively. Dashed line is only an eye guide. Circles represent results of this work.

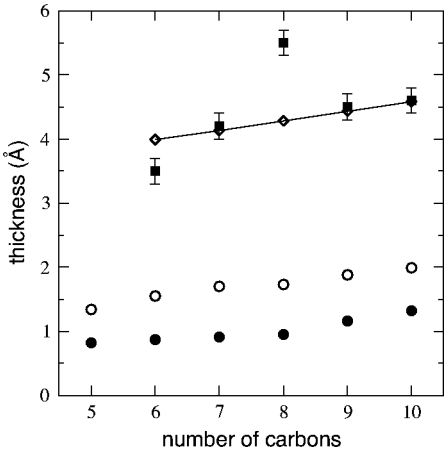

FIG. 7. Interfacial thickness of the liquid-liquid water–*n*-alkane systems as a function of the number of carbons in the *n*-alkane molecule at 298.15 K. Squares and diamonds represent experimental data and theoretical predictions from Mitrinovic *et al.* [10], respectively. Filled and open circles represent results of this work for the intrinsic and total interfacial thicknesses, respectively, based on the ''10-50'' criterion.

In Fig. 7 we present results of this work for the 10-50 intrinsic and total interfacial thickness ($=\sqrt{t_0^2+t_C^2}$) as a function of the number of carbons in the water–*n*-alkane systems. As in the capillary-wave theory of Mitrinovic *et al.* [10], the value for the t_C employed was that obtained from the *n*-alkane density profiles. We compare our results with experimental data for water–*n*-hexane through water–*n*-decane from Mitrinovic *et al.* [10,11] and with the predictions of the capillary-wave theory [10]. From the figure, we can see that the results of this work underpredict the experimental values, but exhibit similar trends to the predictions of the capillary-wave theory [10]; the interfacial thickness grows monotonically with the size of the *n*-alkane chain. Our results have a constant negative deviation of $\sim$2.5 Å from the theoretical predictions and the slope is similar to the experimental results. Experimental data [10] and theoretical predictions agree well for the systems with *n*-heptane, *n*-nonane, and *n*-decane. Figure 8 shows the average ratio profiles of oxygen-hydrogen atoms and CH_3:CH_2 groups along the simulation cell for the system water–*n*-pentane and Fig. 9 for the water–*n*-decane system. These profiles are consecutive averages over 10 ps, with a time between samples of 20 ps.

The agreement between theoretical results and experiments [10] has been proposed as a result of highly ordered *n*-alkane molecules at the interface [38]. As seen in Fig. 3, the small peaks in the *n*-alkane density profile show that *n*-alkane molecules are adsorbed at the interface. However, from Figs. 8 and 9 we do not observe stable layer configurations of *n*-alkane molecules perpendicular to the interface. From the snapshots in Fig. 10, where only *n*-alkane molecules are drawn in views of the *x*-*y* plane of a slab (depth $\Delta z=5$ Å) close to the interface for four configurations separated 100 ps in time, we see a preferred parallel orientation of *n*-alkane molecules close to the interface. This preferred parallel orientation of *n*-alkane molecules at the interface is

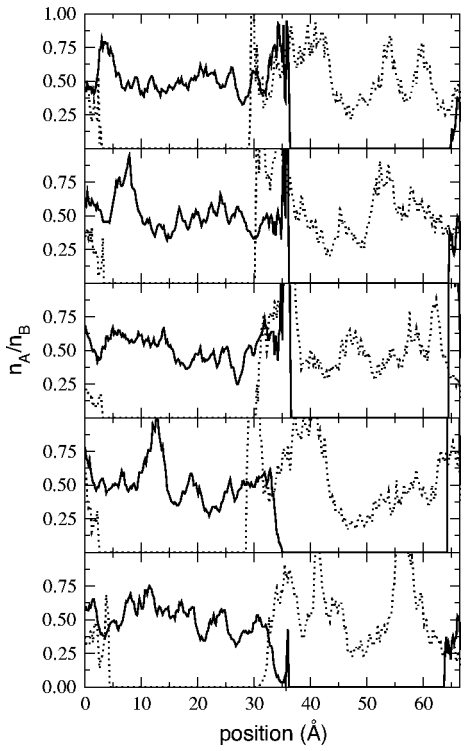

FIG. 8. Hydrogen-oxygen (solid line) and CH_3:CH_2 (dotted line) ratio profiles at different stages of the simulation for the system water–*n*-pentane at 298.15 K. (a) 110 ps, (b) 140 ps, (c) 170 ps, (d) 200 ps, and (e) 230 ps.

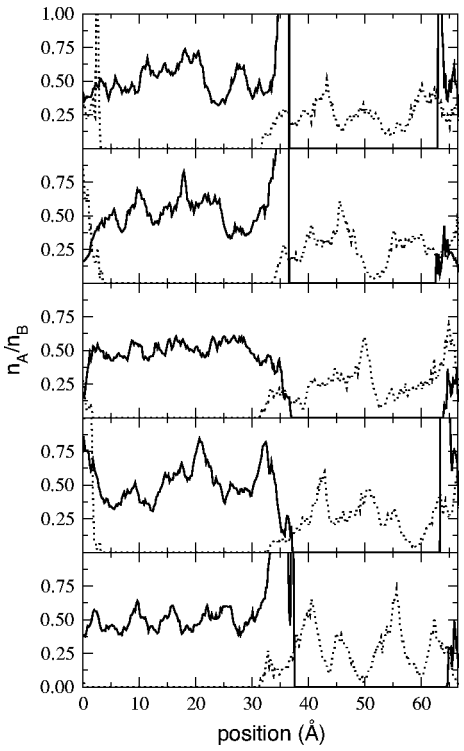

FIG. 9. Hydrogen-oxygen (solid line) and CH_3:CH_2 (dotted line) ratio profiles at different stages of the simulation for the system water–*n*-decane at 298.15 K. (a) 110 ps, (b) 140 ps, (c) 170 ps, (d) 200 ps, and (e) 230 ps.

consistent with the peaks observed in the density profiles, since a parallel orientation will produce better packing of the molecules and yield higher densities for the points close to the interface.

V. LIQUID-LIQUID EQUILIBRIUM RESULTS FOR THE SYSTEM WATER-METHANOL–*n*-PENTANE

This liquid-liquid system was simulated (NVT-MD) using the equilibrated water–*n*-pentane system as the initial configuration. Water molecules were exchanged for methanol molecules to simulate systems with different compositions in the aqueous phase. Density profiles for compositions of 0.059 and 0.681 in the mole fraction of methanol are shown in Figs. 11 and 12, respectively. For low concentrations of methanol, the methanol molecules show a preference to be located at the interface, having peaks of density at the interface. The highest peak ($0.4\ g/cm^3$) was observed for the system with a mole fraction of 0.179. For high concentrations of methanol, the water molecules prefer to be located away from the interface, inside the methanol rich phase, and an incipient concentration of *n*-alkane molecules is observed in the aqueous phase. A snapshot of the system at low concentration of methanol is shown in Fig. 13 (note that only methanol molecules are drawn at full size). As shown in the density profiles, methanol molecules prefer to be located at the interface or inside the aqueous phase (bottom) and no methanol molecules appear in the organic phase (top). When methanol is added to the original water–*n*-pentane system, there is no adsorption of *n*-pentane molecules at the interface for any concentration of methanol. Results of these simulations for interfacial tension as a function of the mole fraction of methanol in the aqueous phase are reported in Table III.

The interfacial tension as a function of the mole fraction of methanol in the aqueous phase is shown in Fig. 14, with experimental data from Hampton *et al.* [39]. Our simulation results agree quantitatively well with the experimental data available, showing that when methanol is added to the system the interfacial tension decreases. This is because methanol molecules behave like very small surfactants; the hydroxyl groups (OH) in the methanol molecule prefer to be located close to the aqueous phase, and methyl groups (CH_3) close to the organic phase. The overall effect is a reordering of the molecules with the inclusion of methanol molecules at the interface and a decrease in the interfacial tension of the system. The binary system methanol–*n*-pentane does not show liquid-liquid coexistence at this temperature, it only shows vapor-liquid coexistence. This is confirmed by Kiser *et al.* [40] who reported that the highest temperature, where liquid-liquid coexistence is observed for methanol–*n*-pentane, is 283.15 K, Orge *et al.* [41] using a group contribution method calculated the vapor-liquid equilibria at 298.15 K, and Carrillo *et al.* [42] also confirmed this showing that for methanol–*n*-alkane systems at 298.15 K, liquid-liquid coexistence occurs only when the *n*-alkane employed has between 6 and 12 carbon atoms. Increasing the concentration of methanol beyond the highest mole fraction reported will allow more *n*-alkane molecules to diffuse to the

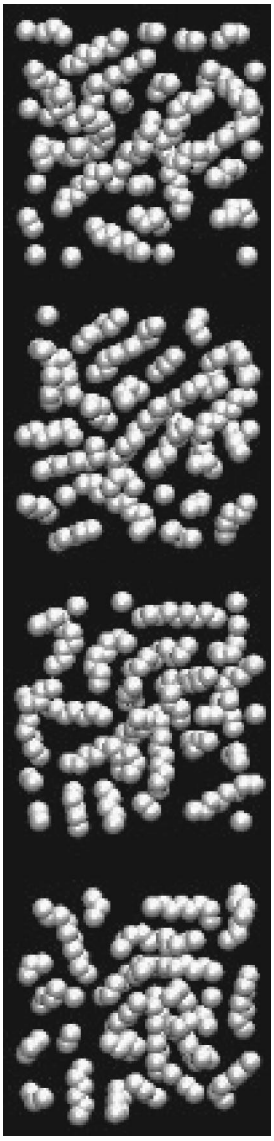

FIG. 10. Snapshots of *n*-alkane molecules in the *x*-*y* plane at the interface (depth $\delta z = 5$ Å) in the system water–*n*-decane at 298.15 K and (a) 300, (b) 400, (c) 500, and (d) 600 ps (from top to bottom).

aqueous phase and when the concentration of methanol is high enough the liquid-liquid system will mix becoming a vapor-liquid system. Studying model Lennard-Jones ternary liquid-liquid systems, Diaz-Herrera *et al.* [17] and Smit [16] found the same behavior when one of the species behaves like surfactant.

VI. CONCLUSIONS

The NERD potential for *n*-alkanes was validated for the prediction of interfacial properties in the vapor-liquid interface using *n*-pentane as an example. The coexisting densities produced by these simulations agree well with the available experimental data and are consistent with previous simulations results for the same model and other models of *n*-alkanes. Unfortunately, there are no experimental or theoretical data to compare the predicted interfacial thickness for *n*-pentane, though we note that the results are similar to, and

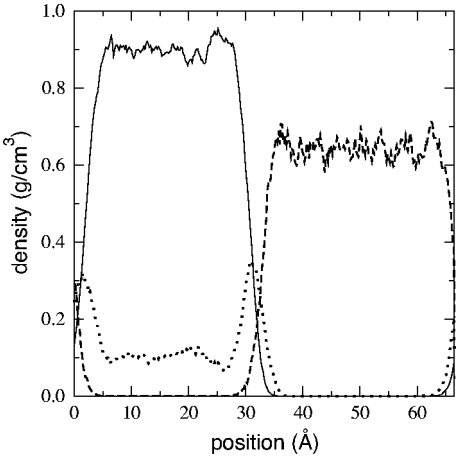

FIG. 11. Density profiles of the liquid-liquid coexistence system water-methanol–*n*-pentane at low concentrations of methanol and 298.15 K. Continuous line is for water, dotted for methanol, and dashed for *n*-pentane.

show the same behavior as previous simulation results of longer *n*-alkanes. The surface tension values predicted by this potential agree quantitatively well with experimental data in the range of temperatures studied.

Results of this work show that, adjusting the number of molecules to reproduce the liquid densities in the direct simulation method of the liquid-liquid coexistence, the potential models can predict quantitatively satisfactory values for the interfacial tension of the water–*n*-alkane systems. Simulation results agree well with experimental data for water–*n*-pentane through water–*n*-decane systems, though the error bar on the predicted results makes the trend of the interfacial tension with chain length unclear. Compared to x-ray reflectivity studies, the results of these simulations underpredict the interfacial thickness as have previous simulation results for pure water. This underprediction of the interfacial thickness is at least in part due to suppression of thermal capillary waves and therefore due to the size of the system employed in this work [33]. Systems with larger in-

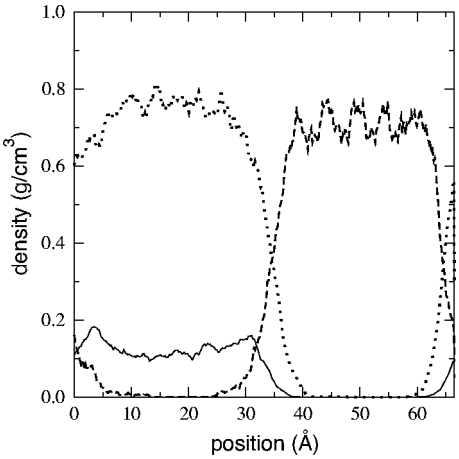

FIG. 12. Density profiles of the liquid-liquid coexistence system water-methanol–*n*-pentane at high concentrations of methanol and 298.15 K. Continuous line is for water, dotted for methanol, and dashed for *n*-pentane.

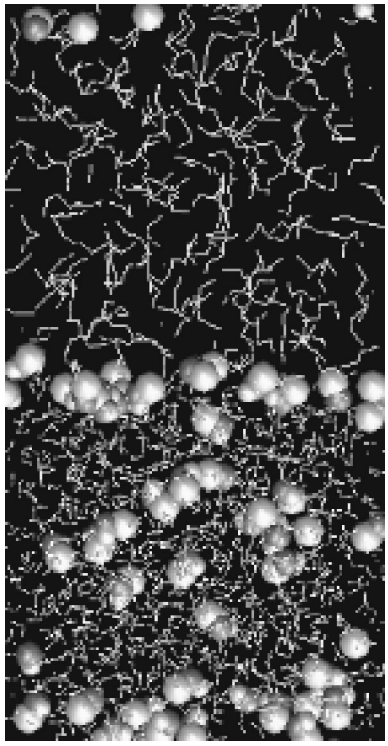

FIG. 13. Snapshot of the system water-methanol–*n*-pentane at 298.15 K with a methanol mole fraction of 0.024 in the aqueous phase (bottom). Only methanol atoms were drawn with their actual size in order to have a clear picture of the system.

terfacial area will produce more exact results for the chosen force fields and we will be performing larger-scale simulations in future work. Previous predictions of the capillary-wave theory agree with experimental interfacial thickness results for some but not all systems and a trend for identifying which systems the theory should agree with experimental data is not clear. There appears to be no formation of stable ordered interfaces, but a preferred parallel orientation of *n*-alkane molecules close to the interface can be observed from snapshots of the system at all times of the simulation. Experimental results for interfacial thickness of water in the vapor-liquid region have an absolute difference ~ 1.1 Å at 298.15 K and our results for the liquid-liquid water–*n*-alkane have an average difference ~ 2.5 Å with experimental data and theoretical predictions. We believe that we have reported consistent experimental and simulation measures of the interfacial thickness, i.e., we have compared liquid-vapor interfacial thicknesses based on the 10-90 criterion used in the corresponding experiments and the liquid-liquid interfacial thicknesses have been calculated based on the 10-50 criterion, which we believe has been used in the corresponding experiments. However, differences between criteria used in the experiment and the simulation could contribute to the differences reported here.

TABLE III. Simulation results for water-methanol–*n*-pentane. Mole fraction of methanol in the aqueous phase x_{met}. Interfacial tension obtained during simulation γ. Numbers between parentheses indicate the precision of the total values.

x_{met}	γ (mN/m)
0.024	41.27 (2.64)
0.059	35.96 (3.27)
0.095	29.88 (3.06)
0.179	24.03 (2.85)
0.384	15.41 (3.16)
0.522	10.11 (3.01)
0.681	7.96 (2.69)

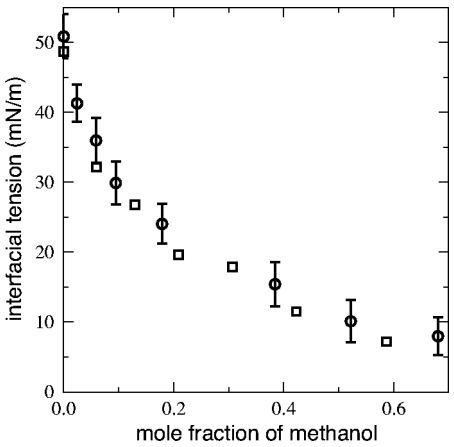

FIG. 14. Interfacial tension of the liquid-liquid system water-methanol-*n*-pentane as a function of the mole fraction of methanol in the aqueous phase at 298.15 K. Squares represent experimental data from Hampton *et al.* [39]. Circles represent results of this work.

By interchanging molecules of water with methanol, we can perform simulations with mole fractions in a wide range of compositions in the aqueous phase of the water-methanol–*n*-pentane system. Methanol is the smallest surfactant for this kind of system; when it is added to the water–*n*-pentane binary mixture it is adsorbed mainly at the interface, decreasing the interfacial tension through a rearrangement of the molecules at the interface. Adsorbed molecules of *n*-alkane at the interface are no longer observed when methanol molecules are present in the system and profiles of these *n*-alkanes are now smooth and continuous without any peak at the interface. Experimental results for the interfacial tension of this system for concentrations of methanol up to mole fractions of 0.6 in the aqueous phase are available and they agree well with the results of this work.

ACKNOWLEDGMENTS

This research was sponsored by the Division of Chemical Sciences, Geosciences, and Biosciences, Office of Basic Energy Sciences, U.S. Department of Energy. This research used resources of the Scalable Intracampus Research Grid (SInRG) Project at the University of Tennessee supported by the National Science Foundation CISE Research Infrastructure Grant No. EIA-9972889. J.L.R. was also supported by Consejo Nacional de Ciencia y Tecnología de México (CONACyT).

[1] L. Stryer, *Protein Structure and Function* (W. H. Freeman, New York, 1995).
[2] K. Arai, F. Kusu, and K. Takamura, in *Liquid-Liquid Interfaces: Theory and Methods*, edited by A.G. Volkov and D.W. Deamer (CRC Press, Boca Raton, FL, 1996), p. 375.
[3] E. Dickinson, S.R. Euston, and C.M. Woskett, Prog. Colloid Polym. Sci. **82**, 65 (1990).
[4] N.M. Morrow, in *Interfacial Phenomena in Petroleum Recovery*, edited by N.M. Morrow (Dekker, New York, 1991), p. 1.
[5] W. Sachs and V. Meyn, Colloids Surf., A **94**, 291 (1995).
[6] A. Goebel and K. Lunkenheimer, Langmuir **13**, 369 (1997).
[7] H. Matsubara, M. Murase, Y.H. Mori, and A. Nagashima, Int. J. Thermophys. **9**, 409 (1988).
[8] A. Braslau, P.S. Pershan, G. Swislow, B.M. Ocko, and J.A. Nielsen, Phys. Rev. A **38**, 2457 (1988).
[9] B.M. Ocko, X.Z. Wu, E.B. Sirota, S.K. Sinha, and M. Deutsch, Phys. Rev. Lett. **72**, 242 (1994).
[10] D.M. Mitrinovic, A.M. Tikhonov, M. Li, Z. Huang, and M.L. Schlossman, Phys. Rev. Lett. **85**, 582 (2000).
[11] D.M. Mitrinovic, Z. Zhang, S.M. Williams, Z. Huang, and M.L. Schlossman, J. Phys. Chem. **103**, 1779 (1999).
[12] H.Y. Jennings and G.H. Newman, Soc. Pet. Eng. J. **11**, 171 (1971).
[13] Y.-X. Zuo and E.H. Stenby, In Situ **22**, 157 (1998).
[14] F.P. Buff, R.A. Lovett, and F.H. Stillinger, Phys. Rev. Lett. **15**, 621 (1965).
[15] M. Sferrazza, C. Xiao, R.A.L. Jones, D.G. Bucknall, J. Webster, and J. Penfold, Phys. Rev. Lett. **78**, 3693 (1997).
[16] B. Smit, Phys. Rev. A **37**, 3431 (1988).
[17] E. Diaz-Herrera, J. Alejandre, G. Ramirez-Santiago, and F. Forstmann, J. Chem. Phys. **110**, 8084 (1999).
[18] I.L. Carpenter and W.J. Hehre, J. Phys. Chem. **94**, 531 (1990).
[19] Y. Zhang, S.E. Feller, B.R. Brooks, and R.W. Pastor, J. Chem. Phys. **103**, 10 252 (1995).
[20] D. Michael and I. Benjamin, J. Phys. Chem. **99**, 1530 (1995).
[21] A.R. van Buuren, S.-J. Marrink, and H.J.C. Berendsen, J. Phys. Chem. **97**, 9206 (1993).
[22] H. Kuhn and H. Rehage, Colloid Polym. Sci. **278**, 114 (2000).
[23] J. Alejandre, D.J. Tildesley, and G.A. Chapela, J. Chem. Phys. **102**, 4574 (1995).
[24] J.L. Rivera, M. Predota, A.A. Chialvo, and P.T. Cummings, Chem. Phys. Lett. **357**, 189 (2002).
[25] J.P. Ryckaert and A. Bellemans, Faraday Discuss. Chem. Soc. **66**, 95 (1978).
[26] H.J.C. Berendsen, J.R. Grigera, and T.P. Straatsma, J. Phys. Chem. **91**, 6269 (1987).
[27] W.L. Jorgensen, J. Am. Chem. Soc. **103**, 341 (1981).
[28] S.K. Nath, F.A. Escobedo, and J.J. de Pablo, J. Chem. Phys. **108**, 9905 (1998).
[29] A. Trokhymchuck and J. Alejandre, J. Chem. Phys. **111**, 8510 (1999).
[30] J. Alejandre, J.L. Rivera, M.A. Mora, and V. de la Garza, J. Phys. Chem. **104**, 1332 (2000).
[31] J.L. Rivera and J. Alejandre, Colloids Surf., A **207**, 223 (2002).
[32] J. Alejandre, D.J. Tildesley, and G.A. Chapela, Mol. Phys. **85**, 651 (1995).
[33] S. Senapati and M.L. Berkowitz, Phys. Rev. Lett. **87**, 176101 (2001).
[34] B.D. Smith and R. Srivastava, *Thermodynamic Data for Pure Compounds: Part A Hydrocarbons and Ketone* (Elsevier, Amsterdam, 1986).
[35] B.A. Grigoryev, B.V. Nemzer, D.S. Kurumov, and J.V. Sengers, Int. J. Thermophys. **13**, 453 (1992).
[36] R.S. Taylor, L.X. Dang, and B.C. Garret, J. Phys. Chem. **100**, 11 720 (1996).
[37] M. Matsumoto and Y. Kataoka, J. Chem. Phys. **88**, 3233 (1988).
[38] J.C. Conboy, J.L. Daschbach, and G.L. Richmond, Appl. Phys. A: Solids Surf. **59**, 623 (1994).
[39] P. Hampton, T. Darde, R. James, and T.H. Wines, Oil Gas J. **99**, 54 (2001).
[40] R.W. Kiser, G.D. Johnson, and M.D. Sheltar, J. Chem. Eng. Data **6**, 338 (1961).
[41] B. Orge, M. Iglesias, A. Rodriguez, J.M. Canosa, and J. Tojo, Fluid Phase Equilibria **133**, 213 (1997).
[42] E. Carrillo, V. Talanquer, and M. Costas, J. Phys. Chem. **100**, 5888 (1996).